Korea-Australia Rheology Journal
Vol. 20, No. 4, December 2008 pp. 253-260

Transient microfluidic approach to the investigation of erythrocyte aggregation: comparison and validation of the method

Jian-Xun Hou and Sehyun Shin*
School of Mechanical Engineering, Korea University, Seoul 136-713, Korea
(Received August 25, 2008; final revision received November 24, 2008)

Abstract

A method based on transient shear flow dynamics of red cell aggregates was developed to investigate reversible re-aggregation processes with decreasing shear flow. In the microchannel-flow aggregometry, the aggregated red blood cells that are subjected to continuously decreasing shear stress in microchannel flow were measured with the use of a laser-scattering technique. Both the laser-backscattered intensity and pressure were simultaneously measured with respect to time, resulting in shear stress ranging from 0~35 Pa for a time period of less than 30 seconds. The time dependent recording of the backscattered light intensity (syllectogram) yielded an upward convex curve with a peak point, which reflected the transition threshold of aggregation in the RBC suspensions. Critical-time and critical-shear stress corresponding to the peak point were examined by varying the initial pressure-differential and the microchannel depth, and these results showed good potential for being used as new aggregation indices. In the present study, these newly proposed indices were also validated by differentiating the effect of fibrinogen on RBC aggregation and then these indices were compared to the conventional indices that were measured by a rotational aggregometer.

Keywords : erythrocyte, aggregation, microfluidic, shear stress

1. Introduction

Red blood cells (RBCs) in normal human blood tend to aggregate spontaneously if the fluid shear forces are below a critical level. Under normal circumstances, the RBC aggregates resemble stacks of coins and therefore, they are called rouleaux. At stasis or under a low shear flow, the rouleaux can grow end-to-end or side-to-end, forming 3D-networks upon completion. Various techniques for measuring RBC aggregation have been developed and they are described elsewhere (Stoltz *et al.*, 1999). The typical techniques are briefly summarized as follows: (i) the light intensity method (Zhao *et al.*, 1999): This technique is based on the principle of recording the light intensity over time and analyzing the transient characteristics of the recorded intensity; (ii) the electrical impedance technique (Pribush *et al.*, 2007): The capacitance and resistance of RBC suspensions are measured in a rectangular channel over time; and (iii) the ultrasonic method (Haider *et al.*, 2004)): This technique adopts ultrasound instead of light and it measures the ultrasonic intensity over time.

Most of the current available techniques that are discussed above provide aggregation indices in terms of an arbitrary unit such as "M" and "M1" indices. Since these indices are strongly dependent on each instrumental characteristic, quantitative comparisons between studies are thus essentially precluded. In order to overcome the difficulty of comparison, a recent study reported the possible use of yield stress as a dimensional aggregation index, which showed a strong correlation with "M" and "M1" indices (Lee *et al.*, 2007). However, since yield stress measurement techniques are subject to experimental or procedural artifacts, most of studies employed an indirect measurement method such as extrapolation method. Therefore, there is need to develop a new method to measure dimensional aggregation index, which may be directly compared between studies.

Furthermore, the previous aggregation indices may not be suitable to interpret the in-vivo RBC aggregation dynamics, since these measurements only allow for the examination of RBC behavior in response to zero-flow or steady-flow conditions. However, an actual in-vivo flow environment is quite different from the zero- or steady-shear condition, and the conventional aggregation parameters may not directly correlate to the in-vivo hemorheological characteristics (Lee *et al.*, 2007). Moreover, the effects of elevated RBC aggregation on the in-vivo hemodynamics are not clear as to whether or not they are helpful for microcirculation (Meiselman and Baskurt, 2006). In our recent study, microfluidic aggregometry was introduced by performing pressure-decreasing rheometry (Shin

*Corresponding author: lexerdshin@korea.ac.kr

et al., 2007), and this requires further interpretation of the proposed indices as well as the measurement principles.

Therefore, the objectives of the present study are to develop dimensional aggregation parameters and to validate them as RBC aggregation indices. Since these newly proposed aggregation indices may be dependent of initial and geometrical conditions, the present study investigates the effects of initial conditions and microchannel dimensions of the microfluidic aggregometer on the proposed aggregation indices. In addition, this study investigates the effect of fibrinogen on RBC aggregation using the proposed indices.

2. Materials and methods

2.1. Sample preparation

Blood was obtained from a healthy volunteer who was not on any medications and who provided informed consent. Venous blood samples were drawn from the antecubital vein and they were collected in Vacutainers (6 ml, BD, Franklin Lakes, NJ, USA) that contained the anticoagulant (K_2)EDTA. In order to obtain RBC suspensions in serum, the blood cells and serum were prepared separately. Whole blood was centrifuged at 2000 × g (2000 times of gravitational acceleration constant) for 10 min. The plasma and buffy-coat were removed. Then, the RBCs were washed three times with isotonic phosphate buffered saline (PBS, pH=7.4, 290 mOsmol/kg). The serum was obtained using Vacutainers (BD, Franklin Lakes, NJ) that contained Gel & Clot Activator and the serum was then introduced to the Vacutainer containing (K_2)EDTA. The washed RBCs were then resuspended either in serum (RIS) or plasma (RIP) with fixed hematocrits at 45%.

2.2. Apparatus and operation

Fig. 1 shows a schematic diagram of the light-backscattering aggregometer using transient microfluidics, which consists of a microchannel, two chambers, vacuum generation mechanism, laser diode, photodiode, and a computer data acquisition system. Detailed description can be found in previous studies (Shin *et al.*, 2007). The vacuum-generating mechanism is connected to a waste sample chamber, which is connected to the microchannel. The length, width and gap of the microchannel were 40 mm, 4 mm and 0.2 mm, respectively. A sample chamber, which was open to the atmosphere, was filled with a test fluid (0.5 ml). When the valve between the vacuum generating system and the waste chamber was opened, the test fluid started to flow through the microchannel and to be collected in the waste chamber as it was being driven by the pressure differential. The test fluid stopped flowing once the pressure differential reached equilibrium with a pressure head. While the test fluid was flowing, pressure differential and backscattered light intensity were simultaneously measured and analyzed.

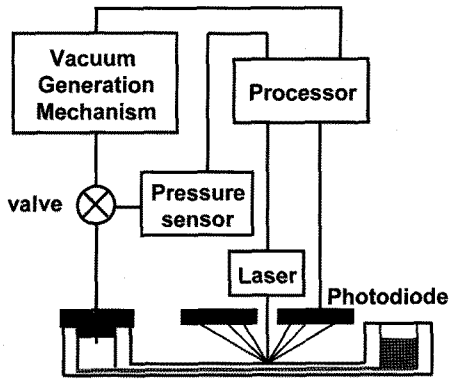

Fig. 1. Schematic of the shear-stress scanning microfluidic aggregometer based on the backscattered light detection system.

While the blood was flowing through the microchannel, a laser beam emitted from the laser diode traversed the diluted RBC suspension and was scattered by the RBCs in the volume. The backscattered light was captured by two photodiodes, which were linked to a computer. When a high pressure differential was initially applied, a strong shear flow occurred through the microchannel and the RBC aggregates started to disaggregate, as was indicated by the corresponding increase in light intensity. As the pressure differential decreased exponentially, the shear flow also decreased and the disaggregated RBCs tended to re-aggregate. Thus, the corresponding light intensity tended to decrease.

In addition to measuring the decreasing pressure-differential process, the intensity of the backscattered light, as a measure of RBC aggregation, was also recorded every 0.01 s. Thus, in the present measurements, the instantaneous-pressure $P(t)$ and instantaneous-light intensity $I(t)$ were simultaneously measured and recorded on a computer data file through an analog-to-digital data acquisition system.

In this study it typically took approximately less than half a minute for the pressure difference to reach an asymptote for blood, as is seen in Fig. 2. In fact, the time to complete a run should vary depending on the type of liquid and the dimensions of the microchannel. It is worth noting that the initial pressure in the vacuum chamber was chosen to produce the maximum shear stress of approximately 30 Pa. The initial vacuum pressure can easily be lowered if it is required to induce a higher shear stress.

2.3. Mathematical principles

A detailed description of the stress-shear rate relation can be found in a previous study (Shin *et al.*, 2005a; Macosko, 1994). A brief description is as follows: In deriving the stress-shear rate relation in microfluidic rheometry, the important assumptions are 1) a fully developed; laminar

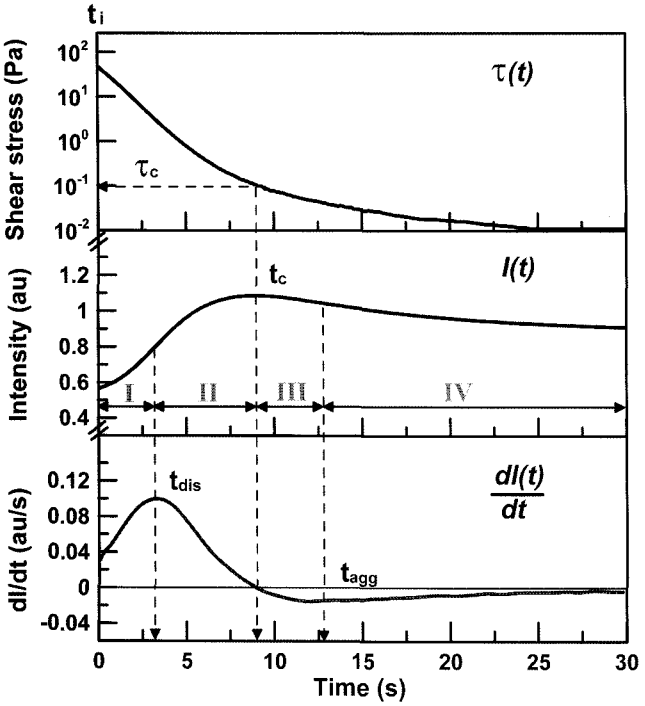

t_i	Initially aggregated
I	Accelerated disaggegation process
II	Decelerated disaggreation process
t_c	Onset of aggregation
III	Accelerated aggregation process
IV	Decelerated aggregation process

Fig. 2. Shear stress and light intensity over time for a blood sample.

flow, isothermal; 2) no slip at the walls; and 3) air in the vacuum chamber as an ideal gas. In this experiment, the instantaneous pressure $P(t)$ was recorded in the computer file.

The measured pressure can be easily converted to a wall shear stress within the microchannel. The pressure differential (ΔP) through a microchannel can be expressed by the following equation:

$$\Delta P(t)=[P_A-P(t)+\rho g\{h_s(t)-h_w(t)\}], \quad (1)$$

where ρ and g are the density of the sample fluid and the gravitational acceleration constant, respectively, P_A and $P(t)$ are the atmospheric and waste-chamber pressures, respectively, and h_s and h_w are the water heads from the datum of the sample and waste chambers, respectively.

The height changes in the waste chamber, $h_w(t)$, can be obtained from:

$$h_w(t)=\frac{V_{liq}(t)}{\pi r_w^2}, \quad (2)$$

where r_w is the radius of the waste chamber and V_{liq} is the liquid volume above the datum. Here, V_{liq} can be determined from the P-V relation that the product of the pressure $P(t)$ and volume $V(t)$ of the air in the waste chamber remains a constant, $P_iV_i=P(t)V(t)$ according to the assumption of the ideal gas law undergoing isothermal process. In fact, during a test, temperature was kept constant within a negligible small range of variation ($\Delta T<0.1^{\circ}C$). Here, the subscript i represents the initial state of the experiment. In addition, since the radii of the sample and waste chambers are the same, the height change in the sample chamber is the same as that in the waste chamber.

Thus, the corresponding wall shear stress is simply obtained from the following equation:

$$\tau_w(t)=\frac{\Delta P(t)H}{(1+H/w)L}, \quad (3)$$

where H, w and L are the height, width and length of the microchannel, respectively. Thus, the wall shear stress can be accurately determined from the instantaneous pressure data $P(t)$. It is worthy to note that shear stress can be determined by pressure measurements, whereas the shear rate requires measuring pressure and flow rate, as described in the previous study (Shin *et al.*, 2005a). The shear rate at the microchannel wall can be obtained from the classical Weissenberg-Rabinowitsch Equation (Macosko, 1994).

$$\dot{\gamma}_w(t)=\left.\frac{dV_z}{dz}\right|_w=\frac{1}{3}\dot{\gamma}_{aw}\left[2+\frac{dlnQ}{dln\,\tau_w}\right], \quad (4)$$

where $=6Q/wH^2$ and $Q(t)=\frac{dV(t)}{dt}=\frac{d}{dt}\left(\frac{P_iV_i}{P(t)}\right)$.

3. Results

Fig. 2 shows the main features of the present measurements, which include light intensity as a function of time and its derivative, and shear stress as a function of time. Since the differential pressure decreases exponentially with respect to time, the corresponding shear stress also decreases as is shown in Fig. 2. Also, the intensity I(t) shows an initial increase, followed by a slow decrease. The initial increase of $I(t)$ is caused by the disaggregation of RBCs due to high-shear flow and the decrease of $I(t)$ is a result of the re-aggregation of RBCs that's associated with low-shear flow (Zhao *et al.*, 1999).

Thus, the maximum point of $I(t)$ in Fig. 2 indicates the starting point of the RBC re-aggregation, and this is strongly dependent on both shear stress and time. The time and shear stress values corresponding to the maximum point of $I(t)$ are defined as the *critical time* (t_c) and the *critical shear stress* (τ_c). Before and after these values of critical time and critical shear stress, there is a critical transition period from dis-aggregation to re-aggregation of the RBCs that's associated with a decreasing shear flow. In order to understand these two parameters, it is worthy to note the first derivative of light intensity with respect to

time, $dI(t)/dt$, as is seen in Fig. 2.

The positive value of $dI(t)/dt$ represents the rate of disaggregation of RBCs and the negative value of $dI(t)/dt$ represents the rate of aggregation. In Fig. 2, the $dI(t)/dt$ value shows a rapid increase and this is followed by an immediate decrease, and $dI(t)/dt$ becomes zero at the critical time. After the critical time, the $dI(t)/dt$ becomes negative, indicating that the RBCs tend to re-aggregate. It is worth noting that the maximum aggregation rate is found at a non-zero shear flow condition rather than a zero-flow one. The newly found parameters should be examined as to whether they can be used as new indices to represent the RBC's aggregation characteristics. Prior to this examination, it is first required that the inherent characteristics of two critical parameters be checked.

It is worthy to recall that the present experiment was under transient flow phenomenon and once-through channel-flow. The cells cannot be aggregated unless the applied shear stress is high and long enough to break-up RBC aggregates via shearing flow. In other words, it required a certain amount of shearing time and flowing distance for aggregates to be disaggregated due to shear flow. This indicates that an abrupt disaggregation from once-through channel flow shearing mechanism cannot be expected. The detection zone, in which the photodiode was mounted, was fixed and the shearing (traveling) time for aggregated cells from the channel entrance to the detection zone is inversely proportional to flow velocity, which is proportional to shear stress. Recall that the shear stress was directly calculated from the pressure difference between the waste chamber and sample chamber.

When a high shear stress is abruptly applied to RBC aggregates, the flow velocity is relatively high and the corresponding shearing time is very short. Thus, it may be disaggregated passing after the detection zone. As the shear stress decreased, the shearing time increased and the disaggregation was also increased. Thus, the corresponding backscattered light intensity increased with decreasing shear stress in Period-I. In this period, both of the rate of disaggregation (dI/dt) and the degree of disaggregation (I) increased, together.

However, as the shear stress decreased further, the rate of disaggregation reached a maximum and started to decrease, even though degree of disaggregation still increased (Period-II). This fact implied that when dI/dt reached maximum, the optimal shearing time was encountered with the corresponding shear stress. Of course, these results may depend on the sensor position and other factors. In this period (II), the shear stress applied on RBC aggregates was still enough to disaggregate whereas the shearing time was sufficiently provided due to decreased shear stress.

As the shear stress decreased further, the rate of disaggregation (dI/dt) crossed zero value and became negative,

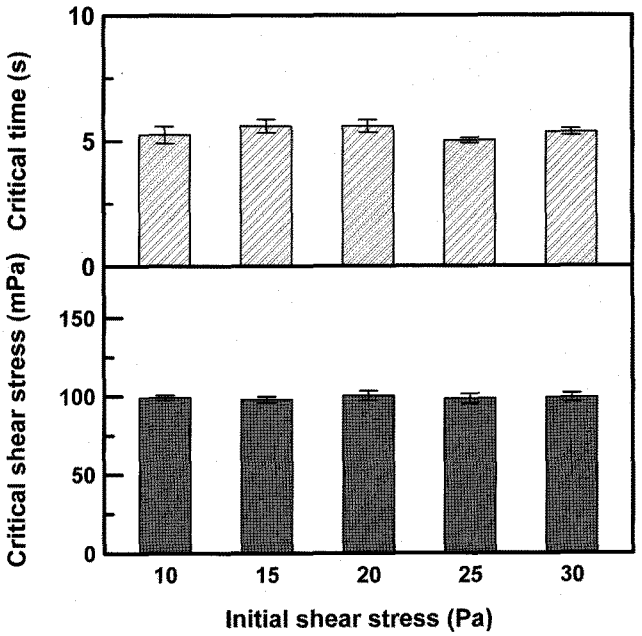

Fig. 3. Variations of critical time and critical shear stress with varying initial conditions.

whereas the degree of aggregation (I) reached a maximum and tended to decrease in Period-III. These result indicated that RBCs started to aggregate beyond the maximum point of I(t), so called *critical point* in the present study. Before and after the critical point, disaggregation stopped and aggregation started due to decrease of shear stress applied on RBC aggregates flowing in the channel flow. Thus, the corresponding backscattered light intensity started to decrease as RBCs tended to aggregate in the Period-III.

The aggregation rate (or negative value of disaggregation rate, dI/dt) is reached maximum as the shear stress further decreased. It is worthy to note that the maximum aggregation rate was observed at non-zero shear condition. This result is coincided with previous results that M1 measured at non-zero shear rate was higher than M measured at stasis.

After reviewing the flow process, the critical time and critical shear stress are examined for various initial shear stress levels between 10 to 30 Pa. Fig. 3 shows the variation of the critical time with the initial shear stress. As the initial shear stress increases, the critical time fluctuates within an acceptable tolerance. The total mean value (MV), standard deviation (SD) and the coefficient of variation (CV) of the critical time are 5.35 s, 0.245 and 4.6%, respectively. Meanwhile, the critical shear stress seen in Fig. 3 is not affected by the initial shear stress. As the initial shear stress is increased up to 30 Pa, the critical shear stress does not vary more than 1.0% (MV = 197.7 mPa, SD = 1.95 mPa). These results imply that both these critical parameters are independent of the initial condition and they are possible aggregation indices that merit further exam-

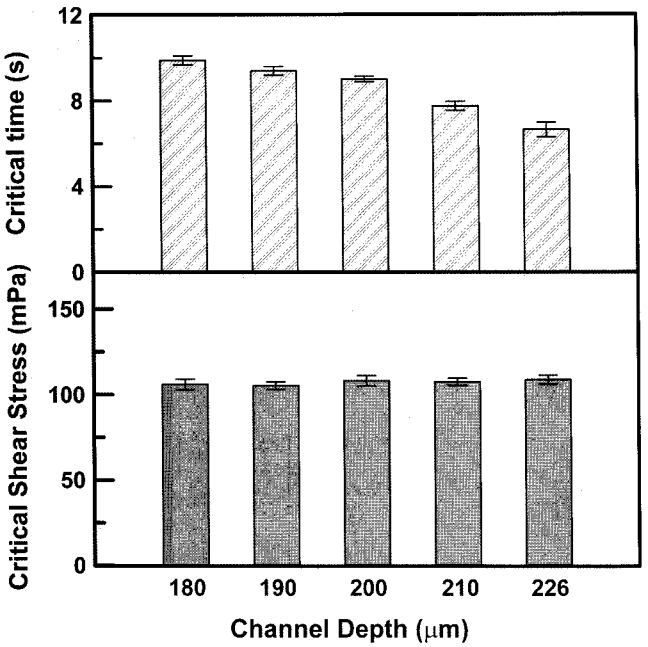

Fig. 4. Variations of critical time and critical shear stress with varying channel depths.

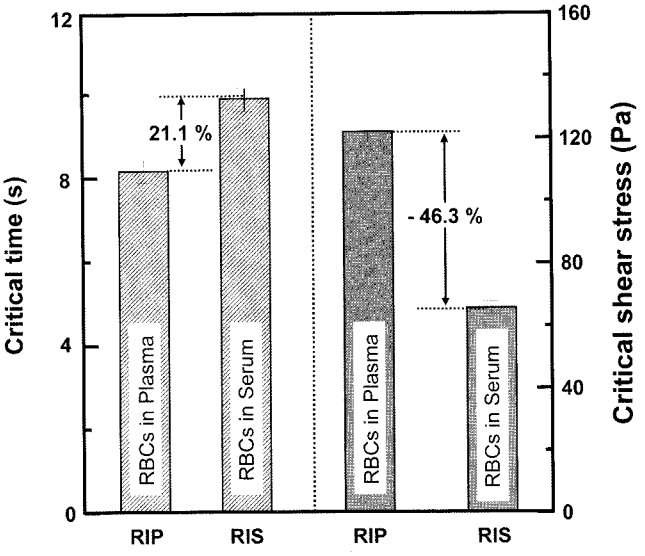

Fig. 5. The effect of the fibrinogen concentration on the critical time and the critical shear stress (RIP: RBC suspensions in Plasma, RIS: RBC suspensions in Serum).

ination.

Fig. 4 shows the effect of the microchannel depth on both the critical time and the critical shear stress. The channel depth dimension varies from 180 to 226 μm with a fixed width and length. As the channel depth increases, the critical time decreases. This result may be expected and it is further interpreted. With an increasing cross-sectional area of a channel, the passing flow rate increases and the time to reach a certain shear stress level becomes shorter. However, the critical shear stress was not affected by the channel dimensions. By increasing the channel depth up to 25%, the critical shear stress does not vary more than 1.4% (MV=107.2 mPa, SD=1.44 mPa). These facts indicate that the critical shear stress is apparently independent of the channel dimensions and it may be proposed as a new aggregation index. The critical time is still a valuable parameter to represent the aggregation characteristics as an auxiliary index.

After careful examination of the proposed parameters, it is found that the critical shear stress can be used as a new index to represent RBC's aggregation characteristics. However, if the channel dimensions are fixed, then the critical time can also be used as an additional index of RBC aggregation. In fact, after examining the initial shear and geometrical conditions, these two variables are fixed. Therefore, two critical parameters will be discussed in the following results.

The effect of fibrinogen on the RBC's aggregation characteristics was examined by the present apparatus and using a conventional aggregometer. Two different blood samples were prepared by modulating the level of fibrinogen in the blood plasma. One sample is a suspension of RBCs in autologous plasma (RIP), which includes 150 mg/dL of fibrinogen. The other one is an RBC suspension in serum (RIS), which does not include any fibrinogen. Both indices showed a strong dependence on the presence of fibrinogen, as is seen in Fig. 5. The elimination of fibrinogen in blood plasma caused a significant reduction in RBC aggregation. The RIS (no fibrinogen) shows a longer critical time (21.1%) and lower critical shear stress (46.3%) than the RIP.

The present measurements were also compared with the conventional aggregation indices that were measured with a rotational aggregometer (LORCA). The detailed RBC-aggregation indices are summarized in Table 1. Aggregation index (AI) is and half time ($t_{1/2}$) can be determined with analyzing light intensity-time syllectogram (Shin *et al.*, 2005b). AI is defined as the ratio of area above the syllectogram to the total area over a 10 s time period, whereas $t_{1/2}$ is defined as the time required to reach a half change of light intensity over 120 s. The higher aggregation occurs, the higher value of AI and the faster of $t_{1/2}$ yield. The present results showed slightly higher values of coefficient of variation (CV) than LORCA. For instance, AI measured with LORCA showed 2.57% of CV, whereas CST did 5.46%. However, the measured results between the LORCA and the present apparatus showed similar tendency for RBC aggregation measurement. When fibrinogen was removed from plasma, both of critical time (t_c) and half time ($t_{1/2}$) for RIS increased and both of critical shear stress (CST) and aggregation index (AI) decreased.

4. Discussion

The present study is a transient analysis of RBC aggre-

Table 1. Comparison of aggregation indices for RBCs-in-plasma (RIP) and RBCs-in-serum (RIS) measured by present apparatus and LORCA

n=10		Present		LORCA	
		CT (s)	CST (mPa)	$t_{1/2}$ (s)	AI (%)
RIP	Mean	7.53	122.05	3.87	50.60
	SD	0.43	6.67	0.15	0.92
	CV	5.71%	5.46%	3.88%	1.82%
RIS	Mean	9.12	65.60	8.13	33.45
	SD	0.23	1.99	0.04	0.86
	CV	2.52%	3.03%	0.49%	2.57%
RV (%)		+21.1	−46.3	110.1	−33.9

gation with using backscattered light, and this indicated there was instantaneous RBC aggregation between cells or the aggregates. Aggregates formed in initial stationary flow condition will tend to disaggregate at higher flow rates due to the increase in shear forces. Because RBC aggregation is a reversible process, reducing the shear forces will result in the reaggregation of RBCs. Since the blood sample stored in the sample chamber is in stationary condition, RBCs aggregates formed before test. When aggregates were applied a high shear stress is applied in the initial period, aggregates tend to disaggregate and thus the corresponding backscattered light intensity increased. The increasing tendency was being kept until the disaggregation process stopped, even though the applied shear stress also decreased. A further decrease of shear stress causes the re-aggregation of RBCs since the inherent aggregating force in the blood overcomes the shear force of the flowing fluid. Thus, the backscattered light intensity falls after the peak intensity is reached and the critical time corresponding to the peak intensity may refer to the start of the re-aggregation process. Since the light intensity is obtained through the channel depth, the critical time represents the bulk mean value.

In fact, the syllectogram shown in Fig. 2 was also observed in our previous study (Shin *et al.*, 2005b). In the design of a pressure-scanning slit viscometer, a transmitted light detection system was added and the syllectogram was simultaneously measured with decreasing. The transmitted light intensity showed a downward convex curve with minimum point, which was indicated as critical shear rate. These results are very similar to the present results having a critical point. It is worthy to note that the blood stored in reservoir was at zero-flow stationary condition and RBCs were highly aggregated, which was identical to the present condition.

The effect of initial state of RBCs was also investigated in our previous study (Shin *et al.*, 2006). Prior to test, blood sample was vibrated at 50 Hz for 30 s and RBCs were disaggregated. After the vibrations suddenly stop, application of decreasing pressure differential allowed the blood sample to flow through the microchannel. The backscattered light intensity showed a plateau of the intensity, which was followed by an exponential decrease of the intensity. The initial plateau was caused by an initial high shearing flow, which did not allow the dispersed RBCs to aggregate. The plateau was kept until the shearing flow was not enough to resist the aggregating force between cells. These previous results are contrast to the present ones without initial vibration, which showed an initial increase of the backscattered light intensity. Thus, these findings may indicate that the critical point reveals the threshold from disaggregation to reaggregation in decreasing shear flow. In addition, we further investigated the effect of initial state of aggregation on the critical shear stress (not shown in the present study). As the initial state of aggregation was varied with increasing rotational speed of micro-stirrer located in the reservoir chamber, the critical parameters were obtained. However, it did not affect the critical shear stress, but the critical time. The corresponding critical shear stress could be the interpreted as a threshold shear stress, which is a variation of the threshold shear rate defined in rotational aggregometer.

It is necessary to check if the measured syllectogram indicates the real RBC aggregation dynamics while the shear stress varies. In general, a complete RBC aggregation used to be considered a multi-step dynamic process including doublet-, rouleaux- and 3D-aggregate formation with finite time constants, respectively. However, if there is any change of RBC aggregation in the multi-step process, the light intensity will also change simultaneously. Thus, the measurement syllectogram (light intensity over time) can be considered for the RBC's aggregation dynamics.

However, a question arises as to whether RBC aggregation can respond to a rapid decay in pressure. If the initial shear stress varies, then the pressure-decay curve and the corresponding time constant of pressure-decay will also vary. However, as shown in Fig. 3, both critical parameters were not affected by the change in the initial shear stress. So, it can be concluded that the critical parameters are not a byproduct of the pressure-decay time constant. The present study assumed that the state of erythrocyte aggregation was at or near to the "quasi-equilibrium" state at each shear stress level in the test flow channel. This assumption should be validated with further systematic investigation of the transient behavior of RBC aggregation.

One may speculate that the dimensions of the rectangular channel used (a depth of 200 micrometers), may limit the formation of normal 3D aggregates. Typical RBC aggregometers have similar dimensions for their present channel gap. For instance, LORCA has a 300 μm gap in a concentric annulus and Myrenne has an approximately 70 μm gap in a cone-plate geometry. They both measure all the 3-D aggregate characteristics, the same as the system presented in this report. Furthermore, even though there may exist radial migration of cells toward the center, some distance from the entrance is required to form a cell-depleted layer. Given the present channel dimensions, there may not be a significant cell-depleted layer.

In the present method of microchannel-flow aggregometry, red cell suspension undergoes a non-uniform shear field. In the channel flow, the shear stress distributes in the range between 0 and the wall shear stress depending on the position in the cross-section. Thus, cells in a microchannel flow may experience various shear levels from zero to the wall-shear stress. However, the present microchannel-flow aggregometry, which is very similar to capillary viscometry, could provide rheological information such as shear stress, shear rate and viscosity by simple measurement of pressure along time (Shin *et al.*, 2005a). A second major advantage for adopting transient-flow aggregometry is that it is very similar to in-vivo pulsatile blood flows in vessels. The pressure-decreasing transient flow characteristics in the present device may yield be transient RBC aggregation, which can be observed in-vivo arterial blood flow. Another reason is that this is relatively inexpensive to build up and simple to operate. Despite of the simplicity, long microchannel or capillary can give highly accurate rheological information (Macosko, 1994).

Even though the critical shear stress represents the hydrodynamic force required to disperse the aggregate, it is a macro-level parameter and a bulk property of a blood sample. Thus, this may not be suitable to depict micro-level changes in the reaggregation process. The syllectogram, obtained from backscattered light signal, might be more sensitive to compared to the critical shear stress and could provide more information on micro-rheological mechanism of aggregation process. However, the critical shear stress provides a dimensional aggregation index, which could be useful to compare their results between studies. Even though the present study tried to validate the newly proposed indices of RBC aggregation, there should be further study on verification of reproducibility with increasing number of tests cases. Furthermore, the present indices may be verified with comparing other conventional aggregation index such as threshold shear rate.

5. Conclusion

The present study investigated the basic characteristics of the newly developed transient microfluidic aggregometry. The critical shear stress was validated as a new RBC aggregation index, which was independent of microchannel geometry and initial conditions. Due to the new aggregation index having dimension, the index measured by various instruments can be directly compared. Furthermore, the transient aggregometry could probe RBC aggregating force with a high resolution capable of detecting the effects of fibrinogen on cell aggregation. Additionally, the present aggregometer may provide an assessment of cell's aggregation property under transient dynamic conditions, which are similar to *in-vivo* blood flow dynamics. Although the transient microfluidic aggregometry was described as an instrument capable of measuring RBC aggregation, further investigation is strongly required to the compare the proposed critical shear stress with the yield stress of blood.

Acknowledgments

This work was supported by grants from the Korea University.

References

Haider, L., P. Snabre and M. Boynard, 2004, Rheology and ultrasound scattering from aggregated red cell suspensions in shear flow, *Biophys J.* **87**, 2322-2334.

Lee, B. K., T. Alexy, R. B. Wenby and H. J. Meiselman, 2007, Red blood cell aggregation quantitated via Myrenne aggregometer and yield shear stress, *Biorheology* **44**, 29-35.

Macosko, C. W., 1994, *Rheology: principles, measurements, and applications*. Wiley-VCH, 237-283(Ch.6).

Meiselman, H. J. and O. K. Baskurt, 2006, Hemorheology and hemodynamics: dove andare?, *Clin Hemorheol Microcirc.* **35**, 37-43.

Pribush, A., L. Hatzkelson, D. Meyerstein and N. Meyerstein, 2007, A novel technique for quantification of erythrocyte aggregation abnormalities in pathophysiological situations, *Clin Hemorheol Microcirc.* **36**, 121-132.

Shin, S., M. S. Park, Y. H. Ku, J. H. Jang and J. S. Suh, 2005a, Simultaneous measurement of red blood cell aggregation and

viscosity: light transmission slit rheometer, *J. Mech. Science Tech.* **19**, 209-215

Shin, S., J. H. Jang, M. S. Park, Y. H. Ku and J. S. Suh, 2005b, A noble RBC aggregometer with vibration-induced disaggregation mechanism, *Korea-Australia Rheology J.* **17**, 9-13

Shin, S., M. S. Park, Y. H. Ku and J. S. Suh, 2006, Shear-dependent aggregation characteristics of red blood cells in a pressure-driven microfluidic channel, *Clin Hemorheol Microcirc.* **34**, 353-361.

Shin, S., J. X. Hou and J. S. Suh, 2007, Measurement of cell aggregation characteristics by analysis of laser-backscattering in a microfluidic rheometry, *Korea-Australia Rheology J.* **19**, 61-66.

Stoltz, J.-F., M. Singh and P. Riha, 1999, *Hemorheology in Practice*, IOS Press.

Zhao, H., X. Wang and J. F. Stoltz, 1999, Comparison of three optical methods to study erythrocyte aggregation, *Clin Hemorheol Microcirc.* **21**, 297-302.